Global NEST Journal, Vol 26, No 8, 05672

Neural network approach to modelling strength characteristics of fly ash, pond ash, and bottom ash integrated geopolymer composites

Rajagopal Shanmugam[1], Rajendran Selvapriya[2], Paramasivam Tamilchelvan[3] and Murugesan Gopinath[2]
[1]Professor, Department of Civil Engineering, Muthayammal Engineering College, Rasipuram.
[2]Assistant Professor, Department of Civil Engineering, Muthayammal Engineering College, Rasipuram.
[3]Assistant Professor, Department of Agricultural Engineering, Muthayammal Engineering College, Rasipuram.
Received: 21/12/2023, Accepted: 11/07/2024, Available online: 17/07/2024
*to whom all correspondence should be addressed: e-mail: shanmugamrgeo@gmail.com
https://doi.org/10.30955/gnj.005672

Graphical abstract

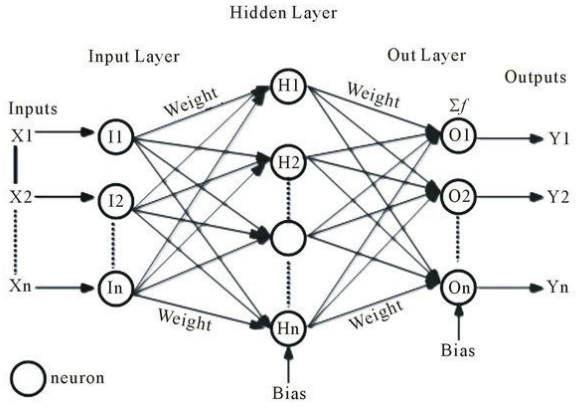

Abstract

Key features for the quality assertion of geopolymer composites are the vital strength characteristics of geopolymer composites. In this work, an artificial neural network data-driven model was employed for predicting 28-day vital strength characteristics for geopolymer composites incorporated with ingredients such as fly ash, manufactured sand, pond ash, bottom ash, coarse aggregate water, sodium hydroxide, and sodium silicate in diverse combinations. In this paper, the ANN model was created using investigational data, and the developed network was trained to fit inputs and the targeted output. ANN modelling was exploited for the prediction of 70 sets of data comprising a training phase of 80%, a testing phase of 10%, and a validation phase of the leftover 10%. To create an artificial neural network, input six parameters to attain one output. Artificial neural networks best exemplified the responses of individual ingredients in composites and established that an artificial neural network is a prospective methodology for predicting vital strength characteristics. It also found that the precision of the outcome primarily depends on the erudition matrix, and the number of data exploited in the training and testing of the network may have had the highest error from -0.0029 to 0.0034 on evaluation.

Keywords: Geo-polymer composites ANN model, compressive, flexural and split tensile, m-sand, pond ash, bottom ash

1. Introduction

As machine learning turns out to be new and further accessible to the common community, academic queries are whirling into critical practical problems. Probably, primarily of the majority, appropriate apprehension is the evaluation of our assurance in trusting machine learning forecasts. In numerous genuine practical studies, it is of paramount significance to evaluate the potential of a machine learning algorithm to generalise, i.e., to afford precise forecasts and predictions on undetected data, depending on the distinctiveness of the target issue or concern. Experimental outcomes reveal the significance of exploiting the idea of the training data in evaluating machine learning generalisation by highlighting the divergence among interpolated and extrapolated forecasts and predictions. In addition to numerous expected correlations, we detect unpredictably feeble associations among the generalisation capability of machine learning mechanisms by employing modelling and the entire set of metrics allied to dimensionality. Geo-polymer composites comprising organic materials are produced through the blending of silicon and aluminium atoms. It was established that. Geo-polymer composites have exemplary properties of mechanical, durability, heat, acid and fire resistance, alkali-silica reaction, eco-friendliness, and easily workability [Anuradha *et al.* 2012; Ahmed *et al.* 2022; Ahmed *et al.* n.d., Bhogayata *et al.* 2021]. It is in vogue for industrial solid waste like fly ash, silica fume, rice husk, metakaolin, and red mud. [Cong *et al.* 2021; Emami & Kamalloo 2012; Gunasekara 2021; Pratap *et al.* 2023; Peng *et al.* 2022], mine waste mud, and slag are materials available that are industrially thrown away by products that can be used for making geo-polymer composites. Out

of the said geopolymeric materials, the primary source is fly ash, reckoned as a foremost resource containing alumino-silicate for soaring characteristic strength attainment [Peng Zhang *et al.* 2022; Sakthieswaran *et al.* 2020]. It was found that enhanced mechanical properties can be attained with geopolymeric gel with a normal density. It was established that lofty compressive, flexural, and split tensile characteristic strengths were attained for sodium-based activating solutions embedded in fly-ash-based geopolymer composites. In the fly-ash-based geopolymer composites, due to chemical actions occurring in the solution stage, microstructures formed. In this paper, pond ash and bottom ash were incorporated as fine aggregate geopolymer composites. [Adesanya *et al.* 2021; Alakara *et al.* 2022; Barbuta *et al.* 2012; Durga]

It is found that diverse factors rely on and influence the compressive, flexural, and split tensile characteristics and strength of geo-polymer composites [Gupta *et al.* 2022; Lau *et al.* 2019; Karimipour *et al.* 2021 & Khan *et al.* 2022]. Owing to the complexity of predicting compressive, flexural, and split tensile characteristic strengths, an artificial neural network was employed to find a solution to this composite problem. A positive tool is cooperating with greatly organized computing rudiments called neurons [Kuppusamy *et al.* 2022; Kong 2022; Nagajothi & Elavenil 2020; Rehman *et al.* 2022; Sharma *et al.* 2023]. It is to point out that artificial neural networks have the primary benefit of prospective learning from the illustrations. It makes a response for unfinished, incomplete, or unfinished assignments, and minimal data or information can be redeemed. It is a potential mechanism or tool for resolving composite tasks and problems with insufficient data [Tingyu *et al.* 2021; Upreti *et al.* n.d.; Wang *et al.* 2022; Yadollahi *et al.* 2015]. It provides a vital approach to training artificial neural network systems from experiment data and develops artificial neural network-based models. For evaluating the performance of materials, an artificial neural network will be deemed a competent model with appropriate data. This will make a replica of the outcome of experiments or investigational data and be capable of making fairly accurate results with its potential [Yaswanth *et al.* 2022; Zhong *et al.* 2024; Zhang *et al.* 2020].

The preceding work of numerous researchers demonstrates that artificial neural network utilization for predicting the properties of geopolymer composites is meager. The artificial neural network was put into use for predicting compressive, flexural, and split tensile characteristic strengths in geopolymer composites and has been conducted by a lot of researchers. [Kuppusamy *et al.* 2022; Sharma *et al.* 2023]. At present, we are doing very scanty research with soft-computing tools in the prediction of geopolymer composite attributes. This study intends to stretch out appropriate models with artificial neural networks to predict the compressive, flexural, and split tensile characteristics and strengths of fly ash, pond ash, bottom ash, and manufactured sand-integrated geopolymer composites.

Faezehossadat Khademi and Sayed Mohammadmehdi Jamal (2016) predicted the compressive strength of recycled aggregate concrete for 28 days. They considered 14 input parameters, both non-dimensional and dimensional. They developed a neural network model, and the input parameters were considered in the network to predict the 28-day compressive strength. They concluded that the ANN model can be used for the strength prediction of concrete with higher accuracy.

Deshpande *et al.* (2014) used ANN to predict the 28-day compressive strength of recycled aggregate concrete. The input parameters were different proportions of cement, recycled aggregates, river sand, coarse aggregates, admixture, and water. They concluded that ANN performs superiorly in considering non-dimensional parameters like the sand-aggregate ratio, water-total materials ratio, aggregate-cement ratio, water-cement ratio, and replacement ratio for the strength prediction of recycled aggregate concrete.

Adriana Trocoli Abdon Dantas *et al.* (2013) developed a model using artificial neural networks (ANN) for predicting the compressive strength of concrete containing construction and demolition waste after 3, 7, 28, and 90 days of curing. In their study, a total of 1178 data points were considered for modeling; 77.76% of the data were considered in the training phase; the remaining 22.24% were considered in the testing phase. The results showed the use of ANN in predicting the compressive strength of construction and demolition waste-incorporated concrete after 3, 7, 28, and 90 days of curing was good and effective.

Duan *et al.* (2013) carried out a study on predicting the compressive strength of recycled aggregate concrete using ANN. They constructed, trained, and tested the ANN model using 146 available sets of data collected from 16 literature sources. 14 input parameters were considered to develop the ANN model. From the test results, they concluded that ANN is more effective in predicting the compressive strength of recycled aggregate concrete.

Akhmad Suryadi *et al.* (2011) predicted the setting time of self-compacting concrete using ANN. A total of 250 different data sets were collected, and the network was trained. They considered 120 data sets in the training, and the remaining data' were considered in the testing and validation phases of the network. The results indicated that the predicted results using ANN showed a dependable correlation between the input data and the targeted output.

Nath *et al.* (2011) developed a model to predict the compressive strength of concrete using a neural network. In order to predict the compressive strength of the concrete, they developed computer code using MATLAB. They concluded that ANN can be effectively used in the prediction of the compressive strength of concrete.

Vahid Alilou and Mohammad Teshnehlab (2009) predicted the 28-day compressive strength using an artificial neural network. They used a multi-input, single-adaptive system to predict the compressive strength. Out of 432 specimens, they used 300 samples data's for training, for validation they considered 66 samples data's and finally for testing they considered 66 samples data's. The simulations were

based on real data from the experimentation, which indicated the cogency of the proposed tool.

Lker Bekir Topc & Mustafa Sardemir (2008) developed a model in artificial neural networks for predicting the splitting tensile and compressive strengths of recycled aggregate and silica fume-added concrete at the ages of 3, 7, 14, 28, 56, and 90 days. Experimental results of 210 specimens cast with 35 different mix proportions were considered for constructing the model. Eight various input parameters were considered. Their test results indicated that the ANN model has strong potential for predicting the splitting tensile and compressive strengths of concrete containing recycled aggregate and silica fume.

From the above literature, it is understood that the geopolymer composite reveals excellent properties in all aspects when compared to ordinary Portland cement concrete. Due to the unavailability of large quantities of natural sand, pond ash, bottom ash, and M-sand are partially replaced by natural sand. Observing the merits of geopolymer composite over ordinary Portland cement concrete from the literature tour, experimental research work has been conducted on the partial replacement of M-sand and bottom ash for natural sand for producing geopolymer concrete. Furthermore, it is clear from the existing literature collections that no such work has been done on pond ash, bottom ash, or M-sand in geopolymer composites. This research also makes an attempt at curing specimens at ambient temperature. The results of the different tests are presented in the following chapters, and the compliance of geopolymer composites in structural applications in the Indian context is verified.

Figure 1. Pictorial representation of fly ash

Over fitting is an elementary concern in organised machine learning, which averts from absolutely generalising the models to fine-tuning experimental data on training data as well as undetected data on testing sets. Due to the limited size of the training set and the difficulty of classifiers, over fitting occurs. To diminish the effect of overfitting, a diverse approach is projected to tackle this problem:

1) It will be addressed by launching an "early-stopping" strategy; thereby, over fitting can be prevented by stopping training earlier than the potential or recital ends optimisation;
2) In the training set, a "network reduction" approach is to be adopted to eliminate the noises in the training set;
3) For complex models, it can be tackled by adopting a “data expansion" approach to perfect the hyper-parameters set with a vast quantity of data;

2. Materials

2.1. Fly Ash

Class F-type fly ash shown in Figure 1 was used as binder in this research, which is obtained from a thermal power station located in Mettur, Tamil Nadu. Table 1 presents the physical and chemical properties of Class F fly ash.

Table1. Physical and chemical attributes of fly ash

Attributes	Test results
Specific Gravity	2.295
Fineness	437m^2/kg
SiO_2	60.39%
Al_2O_3	24.07%
Fe_2O_3	4.07%
$SiO_2 + Al_2O_3 + Fe_2O_3$	88.34%
MgO	1.23%
CaO	2.47%
SO_3	2.66
Alkali	2.48%
LOI	1.22%

2.2. Pond ash

Pond ash used in this work, with the following characteristics, was procured from nearby sources: [Ting-Yu *et al.* 2020; Zhong *et al.* 2023] Its grading was found in Zone III of IS 383-1970. Attributes of pond ash were illustrated in Table 2, and Figure 2 shows the particle size distribution of pond ash.

Figure2. Pictorial representation of pond ash

Table2. Physical and chemical attributes of pond ash

Attributes	Test results
Specific Gravity	2.140
Water Absorption	0.720
Fineness Modulus	2.670
SiO_2	48.23
Al_2O_3	14.69
Fe_2O_3	0.62
CaO	1.84
MgO	0.84
CO_2	31.45
LOI	5.13

2.3. M -Sand

M-sands are crushed river sands produced from hard granite stones that are cubical-shaped with grounded edges, washed, and graded with consistency to be used as a substitute for river sand. Figure 3 shows the pictorial representation of M-Sand. The properties and grading of M-Sand are presented in Tables 3 and 4, respectively.

Figure3. Pictorial representation of M-Sand

Figure 4. Pictorial representation of bottom ash

Table 3. Physical and chemical attributes of M -Sand

Sl.No.	Attributes	Test values
1.	Specific gravity	2.62
2.	Fineness modulus	2.85
3.	Water absorption (%)	0.82
4.	SiO_2	67.52
5.	Al_2O_3	15.33
6.	Fe_2O_3	3 5.48
7.	CaO	3.15
8.	Na_2O,K_2O	4.11
9.	LOI	3.15

Table 4. Grading of M-Sand

IS Sieve	Weight retained (gm)	Cumulative Weight retained (gm)	% Cumulative Weight retained	% Passing	(Zone III)
4.75 mm	92	92	9.2	90.8	90-100
2.36 mm	69	161	16.1	83.9	85-100
1.18 mm	91	252	25.2	74.8	75-100
600 micron	194	446	44.6	55.4	60-79
300 micron	402	848	84.8	15.2	12-40
150 micron	129	977	97.7	2.3	0-10
Pan	23	1000	100	0	-

Table 5. Physical and chemical attributes of bottom ash

Sl.No.	Attributes	Test values
1.	Specific gravity	2.32
2.	Fineness modulus	2.675
3.	Water absorption (%)	0.82
4	SiO_2	45.62
5	Al_2O_3	18.22
6	Fe_2O	38.70
7	CaO	8.14
8	MgO	3.82
9	SO_3	0.46
10	K_2O	2.07
11	Na_2O	0.27
12	TiO_2	0.96
13	P_2O	5.96
14	SiO_2, $Al2O_3$, Fe_2O_3	92.54
15	LOI	3.85

Table 6. Grading of bottom ash

IS Sieve	Weight retained (gm)	Cumulative Weight retained (gm)	% Cumulative Weight retained	% Passing
4.75 mm	108	108	10.8	89.2
2.36 mm	114	222	22.2	77.8
1.18 mm	176	398	39.8	60.2

600 micron	342	740	74	26
300 micron	164	904	90.4	9.6
150 micron	79	983	98.3	1.7
Pan	17	1000	100	0

2.4. Bottom Ash

The bottom ash used in this research was collected from a thermal power station in Mettur, Tamil Nadu. In wet conditions, bottom ash was obtained as coarser in size. Figure 4. shows the pictorial representation of bottom ash.

Bottom ash particles were received from the boilers and possessed a glassy structure and shape that was angular. The properties and grading of bottom ash are presented in Tables 5 and 6, respectively.

Table 7. Physical and chemical attributes of coarse aggregate

Sl.No.	Attributes	Test values
1.	Specific gravity	2.67
2.	Fineness modulus	6.31
3.	Water absorption (%)	0.68
4.	SiO	2 75
5.	Al2O3	15.24
6.	Fe2O3	2.44
7.	MnO	0.09
8.	CaO	0.98
9.	MgO	0.09
10.	Na_2O	1.57
11.	K_2O	2.49
12.	TiO_2	0.03
13.	P_2O_5	0.23

Table 8. Grading of coarse aggregate

IS Sieve	Weight retained (gm)	Cumulative Weight retained (gm)	% Cumulative Weight retained	% Passing
20 mm	238	238	4.76	95.24
10 mm	3480	3718	74.36	25.64
4.75 mm	1172	4890	97.80	2.20
2.36 mm	50	4940	98.80	1.20
1.18 mm	10	4950	99.00	1.0
600 micron	30	4980	99.60	0.40
300 micron	10	4990	99.80	0.20
150 micron	5	4995	99.90	0.10
Pan	5	5000	100	0

Table 9. Physical and chemical attributes of sodium hydroxide

Sl.No.	Attributes	Value
1.	Colour	Colour less
2.	Specific gravity	1.46
3.	pH	13
4.	Sodium Carbonate (Na2CO3)	2%
5.	Chloride (Cl)	0.01%
6.	Sulphate (SO3)	0.05%
7	Potassium (K)	0.1%
8	Silicate (SiO2)	0.05%
9	Zinc (Zn)	0.02%
10.	Heavy metals (as Pb)	0.002%
11	Iron (Fe)	0.002%
12	Minimum Assay	97.0%
13	Molarity	30

Table 10. Physical and chemical properties of sodium silicate

Sl.No.	Parameters	Test results
1.	Na_2O	15.5%
2.	SiO_2	31.12%
3.	H_2O	53.08%

4.	Appearance	Liquid (Gel)
5.	Colour	Light yellow
6.	Boiling Point	101.2^{o}C
7.	Molecular Weight	183.22 g
8.	Specific Gravity	1.65

2.5. Coarse aggregate

Aggregates of 20 mm in size were used as coarse aggregate for the preparation of geopolymer composite specimens in this research. Figure 5 shows the coarse aggregate used in this research. The fineness modulus, specific gravity, and water absorption of coarse aggregate were determined as per IS 2386: 1963 (Part 1) and (Part 3). The tested values are shown in Table 7. The sieve analysis test was done as per IS 2386 (Part 1)-1963. The gradation value of coarse aggregate is shown in Table 8.

Figure 5. Pictorial representation of coarse aggregate

Figure 6. Pictorial representation of sodium hydroxide in pellet form

2.6. Sodium Hydroxide

Generally, sodium hydroxides are available in a solid state by means of pellets and flakes. In this research, sodium hydroxide in pellet form with 97-98% purity, which is commercially available, is used. The physical and chemical properties of sodium hydroxide pellets are presented in Table 9. Figure 6 shows sodium hydroxide in pellet form.

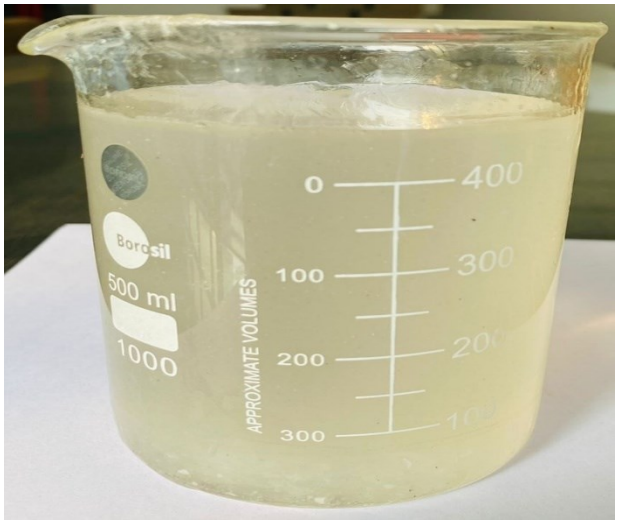

Figure 7. Pictorial representation of sodium silicate in jel form

2.7. Sodium Silicate

Sodium silicate, also known as water glass or liquid glass, is available in liquid (gel) form. In the present investigation, the ratio between Na_2SiO_3 and SiO_2 is used as 2. As per the manufacturer, silicate was supplied to the detergent company and textile industry as a bonding agent. The same sodium silicate was used for the preparation of an alkaline activator solution for producing geopolymer concrete specimens. The chemical properties and the physical properties of the silicates are presented in Table 10. Figure 7 shows the sodium silicate in jel form used in this research.

The strength characteristics of geo-polymer composites are deemed vital factors for the quality assertion of geo-polymer composites. In this research, a data-driven model, i.e., an artificial neural network (ANN), was evolved to predict the 28-day compressive, flexural, and split tensile strength characteristics of fly ash, M-sand, pond ash, and bottom ash integrated geo-polymer composites.

Table 11. Shows data on diverse ingredients as inputs for geopolymer composites in kg/m^3.

Mix ID	Fly ash	M-sand	Pond ash	Bottom ash	Coarse aggregate	Water	NaOH	Na_2SiO_3
D-1	425.25	645.45	0	0	1259.55	36.75	58.95	142.15
D -2	480.95	583.45	0	0	1118.45	44.65	63.75	163.15
D -3	480.25	620.55	0	0	1108.45	44.25	63.75	163.15
D -4	554.75	560.45	0	0	1002.25	14.25	68.85	170.25
D -5	543.95	535.75	0	0	988.50	28.45	72.45	180.75
D -6	585.65	535.45	0	0	832.85	28.35	72.25	180.50
D -7	554.75	450.25	0	0	929.15	14.25	74.95	184.60
D -8	585.65	576.25	0	0	1018.05	12.75	78.25	200.50
D -9	552.50	567.50	0	0	987.75	44.35	78.25	190.50
D -10	555.25	550.85	0	0	957.95	44.25	68.5	171.15
D -11	638.25	534.25	0	0	929.15	44.25	68.5	171.15

D -12	510.75	567.15	0	0	882.25	28.35	68.5	171.15
D -13	585.65	586.25	0	0	907.55	28.35	79.8	204.65
D -14	483.75	585.45	0	0	1018.5	28.35	70.2	175.50
D -15	554.75	535.45	0	0	832.85	14.25	73.25	180.30
D -16	583.75	535.45	0	0	882.25	14.25	73.25	180.30
D -17	564.75	543.25	0	0	832.85	14.25	73.85	185.60
D -18	585.65	515.25	0	0	902.25	14.25	73.85	185.65
D -19	584.75	535.25	0	0	798.25	28.35	80.85	204.25
D -20	585.65	534.65	0	0	883.25	12.75	80.85	204.25
D -21	570.85	535.25	0	0	883.25	28.35	78.24	195.65
D -22	547.25	567.15	0	0	957.95	44.25	68.50	171.15
D -23	585.65	535.45	0	0	832.85	12.75	82.25	210.50
D -24	564.75	535.45	0	0	832.8	28.35	82.25	205.50
D -25	519.75	613.25	0	0	964.25	44.25	68.50	171.15
D -26	585.25	550.85	0	0	907.50	14.25	82.85	210.65
D -27	585.25	585.45	0	0	1018.15	28.35	82.85	210.65
D -28	585.25	567.15	0	0	957.95	14.25	83.25	207.35
D -29	638.25	545.0	0	0	882.25	12.75	68.5	171.15
D -30	485.65	613.0	0	0	1218.25	58.50	65.25	167.35
D -31	455.25	608.17	613.25	0	1249.5	58.85	145.25	145.25
D -32	480.75	610.25	608.15	0	1118.15	63.50	163.15	163.15
D -33	480.25	589.97	610.25	0	1108.15	63.50	163.15	163.15
D -34	554.75	615.67	589.95	0	1002.25	68.80	170.25	170.25
D -35	543.75	572.27	615.65	0	987.50	72.25	180.50	180.55
D -36	585.65	613.25	572.25	0	832.85	72.25	180.50	180.50
D -37	554.75	670.87	613.5	0	929.15	74.85	184.65	184.65
D -38	585.65	589.95	670.85	0	1018.55	78.25	200.50	200.50
D -39	552.65	572.27	589.95	0	987.55	78.25	190.50	190.50
D 40	555.25	615.67	572.25	0	957.95	68.50	171.15	171.15
D -41	638.25	652.17	615.65	0	929.15	68.50	171.15	171.15
D -42	510.75	670.85	652.15	0	882.25	68.50	171.15	171.15
D -43	585.65	572.27	670.85	0	907.55	79.80	204.6	204.65
D -44	483.75	613.25	572.25	0	1018.5	70.25	175.5	175.50
D -45	554.75	615.67	613.25	0	832.85	73.25	180.3	180.35
D -46	583.75	652.17	652.1	0	882.25	73.25	180.3	180.35
D -47	564.75	670.85	615.6	0	832.85	73.85	185.6	185.65
D -48	585.65	572.27	589.9	0	902.25	73.85	185.6	185.65
D -49	584.75	613.25	572.2	0	798.25	80.85	204.6	204.25
D -50	585.65	652.17	670.8	0	883.25	80.85	204.6	204.25
D -51	570.85	615.68	572.2	0	883.25	78.24	195.6	195.50
D -52	547.55	589.94	608.1	0	957.95	68.55	171.1	171.25
D -53	585.65	572.27	615.6	0	832.85	82.25	210.5	210.25
D -54	564.75	670.87	615.6	0	832.85	82.15	205.5	205.25
D -55	519.77	572.28	625.7	0	964.25	68.55	171.1	171.50
D -56	585.25	608.17	572.2	0	907.55	82.85	210.6	210.75
D -57	585.40	615.67	550.1	0	1018.5	82.85	210.6	210.75
D -58	585.40	615.65	572.2	0	957.95	83.25	207.3	207.35
D -59	638.25	625.74	613	0	882.25	68.55	171.1	171.15
D -60	485.65	572.24	713.25	0	1218.25	65	167.3	167.35
D -61	405.25	0	136.65	0	1218.25	108.35	72.88	72.88
D -62	405.25	0	273.35	0	1218.25	108.35	72.88	72.88
D -63	405.25	0	409.95	0	1218.25	108.35	72.88	72.88
D 64	405.25	0	546.50	0	1218.25	108.35	72.88	72.88
D -65	40.25	0	683.15	0	1218.25	108.35	72.88	72.88
D -66	405.25	0	0	68.35	1218.25	108.35	72.88	72.88
D -67	405.25	0	0	136.65	1218.25	108.35	72.88	72.88
D -68	405.25	0	0	204.97	1218.25	108.35	7288	72.88
D -69	405.25	0	0	273.25	1218.25	108.35	72.88	72.88
D -70	405.25	0	0	341.55	1218.25	108.35	72.88	72.88

3. Sample preparation and testing

Diverse ingredients were weighed and taken for sampling. The initially required quantity of fly ash, M-sand, pond ash, and bottom ash integrated geo-polymer composites was mixed thoroughly. An activating solution comprising sodium hydroxide and sodium silicate, mixed one day earlier for casting, was added to the dry ingredients. All the

ingredients were thoroughly muddled. The ratio between fly ash and alkaline solution was kept at 2.5, and the molarity of NaOH used in this investigation was 12 molar. The ratio between fly ash and alkaline Solution ratio as 2.5 and molarity of NaOH was used in this investigation was 12molar.Specimen cubes of size 100mm x 100mm x 100mm, cylinders with a 100mm diameter x 300mm, and prisms measuring 100mm x 100mm x 750mm were moulded and cured for 28 days at an accustomed temperature. The next day, specimens were kept for curing after being removed from mould. By conducting compressive, split tensile, and flexural tests, the characteristics of the geopolymer composite were determined.

3.1. Data collection

In this work, acquired data containing the outcomes of various experiments utilized as input about geopolymer composites contain various mix proportions for training artificial neural network models. It was confirmed that they are resources embedded with silica and alumina through the supply of oxygen to formulate geopolymer composites. This paper is uniting as much data from 70 sets comprising geopolymer composite ingredients (fly ash, manufactured sand, pond ash, and bottom ash) about compressive, flexural, and split tensile characteristic strengths in geopolymer composites congregated from the outcomes of various experiments for training network models. [Sakthieswaran et al 2020] Data on diverse combinations of fly ash, pond ash, and bottom ash-integrated geopolymer composites are illustrated in Table 11. Different combinations of mixes were shown with mixes of identity prefixed with D and numbered serially as D1, D2, and D3, etc. The most advantageous molarity was ascertained as 12 for geopolymer composites. The same was espoused in geopolymer composites with diverse ingredients utilized in training artificial neural network models.

Figure 8. Compression strength characteristics test on geopolymer concrete cubes

3.2. Compressive strength characteristics test

The compressive strength of fly ash, M-sand, pond ash, and bottom ash integrated geo-polymer composites is deemed the prime factor for quality assurance. A compression strength test was carried out as per IS 516-1959 to find out the compressive strength of geo-polymer composites incorporated with fly ash, M-sand, pond ash, and bottom ash integrated appropriately. The compressive characteristics and strength of geo-polymer composites were tested at the ages of 7 and 28. Figure 8 shows the test setup for the compression strength test.

3.3. Split tensile strength characteristics test

Split tensile testing of fly ash, M-sand, pond ash, and bottom ash integrated geo-polymer composites was carried out as per the test procedure specified in IS 516-1959. After 7 and 28 days of curing, the split tensile strength of geopolymer concrete was determined. Figure 9 shows the test setup for the split tensile strength test.

Figure 9. Split tensile strength characteristics test on geopolymer composite cylinder

3.4. Flexural strength characteristics test

A flexural strength test was performed as per IS 516-1959 to find out the flexural strength of fly ash, M-sand, pond ash, and bottom ash integrated geo-polymer composites. The system of loading used to determine the flexural strength was central point loading. Figure 10 shows the test setup for the flexural strength test.

Figure 10. Flexural strength characteristics tests on geopolymer concrete prisms

4. Neural network modelling

At present, we have various neural network modelling architectures; hence, it is vital to keep the appended concepts in mind when choosing an appropriate neural network. Figure 11 shows the flow chart of the Levenberg-Marquardt algorithm used in this research. Figure 12 shows the flow chart of the artificial neural network used in this research.

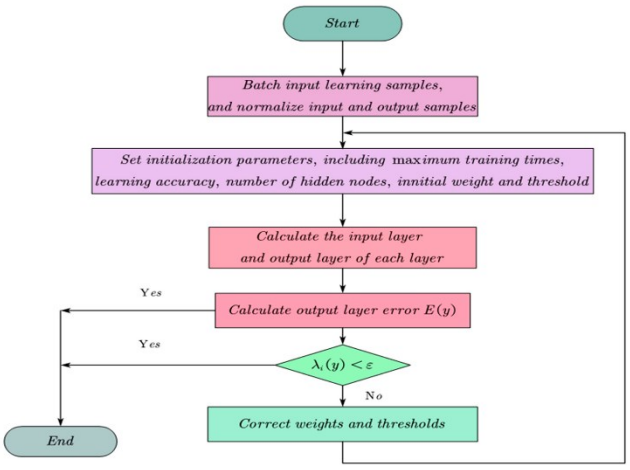

Figure 11. A flow chart of the Levenberg-Marquardt algorithm

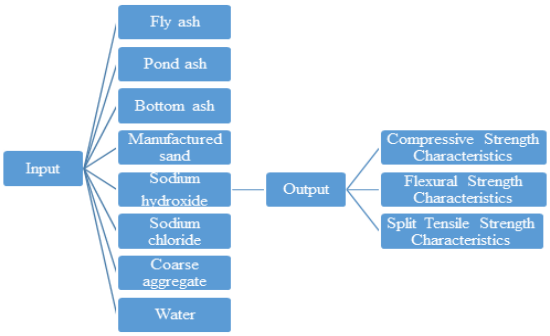

Figure 12. A flow chart of an artificial neural network

The compressive, flexural, and split tensile strength characteristics of geopolymer composites integrated with fly ash, M-sand, pond ash, and bottom ash were evolved as outputs for the respective neural network models. The results attained in the training, testing, and validation phases steadily demonstrate the potential use of ANN to predict the compressive, split tensile, and flexural strength characteristics of geopolymer composites integrated with fly ash, M-sand, pond ash, and bottom ash.

- The input nodes of the neural network model are chosen from a comprehensive number of free-spirited factors.
- 80% of input nodes are fixed as the base for hidden node numbers.
- Hidden layers were reduced to evade the training period with a longer duration.
- To avoid overstating, the number of neurons was fixed adequately.
- Input data sets of the first 30 (1–30) with ingredients of fly ash, manufactured sand, sodium hydroxide, sodium chloride, coarse aggregate, and water
- Input data sets of the next 30 (31–60) with ingredients of fly ash, pond ash, manufactured sand, sodium hydroxide, sodium chloride, coarse aggregate, and water.
- Input data sets of the next 5 (61-65) with ingredients of fly ash, pond ash, sodium hydroxide, sodium chloride, coarse aggregate, and water.
- Input data sets of the last 5 (66–70) with ingredients of fly ash, bottom ash, sodium hydroxide, sodium chloride, coarse aggregate, and water.

Compressive, flexural, and split tensile strength characteristics for all 70 sets of output data.

At present, we are using MATLAB software, which is a widespread technique for training neural networks. As MATLAB is a user-friendly method, we prefer it. For training neural networks, Levenberg-Marquardt, the most common algorithm in vogue, was adopted. Here, the potential outcome was evaluated based on the coefficient and determination of the mean absolute percentage deviation [MAPD] [Tingyu *et al.* n.d.].

Typically, neural networks consist of three layers: the input layer, or initial data for the neural network; hidden layers, or intermediate layers, between the input and output layers and the place where all the computation is done; and the output layer, which produces the result for given inputs. In this work, we are relating the hidden layer to other layers using the notions of weights, bias, and activation tasks. Every layer comprises abundant neurons. The dataset provides input for every neuron. Output can be predicted by activating weighed inputs and processing them together. The development of a neural network using MATLAB has been illustrated in Figure 13.

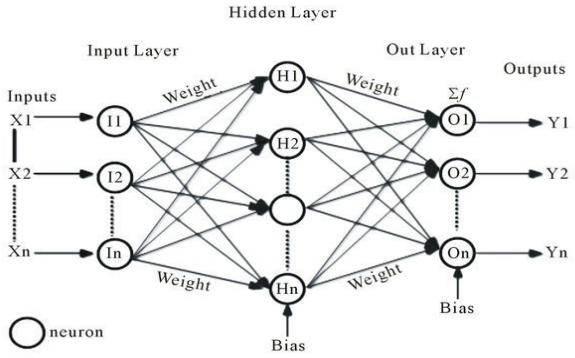

Figure 13. ANN model configurations

The various steps involved in developing the ANN model for predicting the 28-day compressive, flexural, and split tensile strength characteristics of fly ash, M-sand, pond ash, and bottom ash integrated geopolymer composites are explained as follows: Large data sets were utilized in this model; therefore, a neural fitting tool was used in analogous function approximation. MATLAB 9.1 software was utilised to develop the ANN model.

5. Training and testing of neural networks

In this paper, artificial neural network models were evaluated with several inputs comprising 6 as the input layer, several nodes comprising 12 as the hidden layer, and several outputs comprising 1 node as the output layer. Generally, only one hidden layer was chosen in artificial neural network models in many accomplishments. Hit-and-miss or repetition techniques adopted in the process of prediction for perpetual and meticulousness in creating neural networks Experiments with hidden nodes six, eight, nine, and ten were attempted in artificial neural network models. On assessment, the best recital was attained with hidden nodes having twenty-four coupled with a mean absolute percentage deviation [MAPD].

In this research, 12 neurons were assigned to the hidden layer to train the model. The training ratio was assigned as

80%, and the test ratio was assigned as 10%. The remaining 10% was assigned as a validity ratio. The structure of the ANN model used to predict the compressive strength is shown in Figure 14.

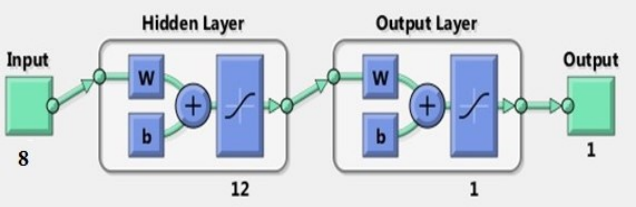

Figure 14. Structure of the ANN model for compressive strength characteristics prediction

An ANN model was developed to predict the flexural strength characteristics of Fly ash, M-sand, pond ash, and bottom ash are integrated geopolymer composites. The basic approach to developing ANN-based models is to train ANN systems with data obtained from trials. If appropriate information is acquired, then the trained ANN systems will be deemed a qualified model to weigh the behaviour of materials. Such systems are not only able to imitate the investigational outcome, but they can also fairly accurately predict the outcome of other investigations through their capabilities.

In order to predict the flexural strength characteristics, a total of 24 neurons were assigned to the hidden layer to train the model. The training ratio was assigned as 80%, and the test ratio was assigned as 10%. The remaining 10% was assigned as a validity ratio. The structure of the ANN model used to predict the flexural strength characteristics is shown in Figure 15.

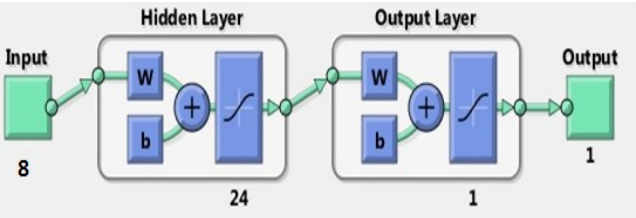

Figure 15. Structure of the ANN model for flexural strength characteristics prediction

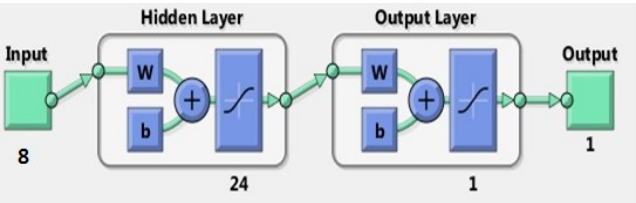

Figure16. Structure of the ANN model for split strength characteristics prediction

An ANN model was developed to predict the split tensile strength characteristics of Fly ash, M-sand, pond ash, and bottom ash are integrated geopolymer composites. Totally, 24 neurons were assigned to the hidden layer to train the model. The training ratio was assigned as 80%, and the test ratio was assigned as 10%. The remaining 10% was assigned as a validity ratio. The structure of the ANN model used to predict the split tensile strength characteristics is shown in Figure 16.

In neural networks, inputs were trained aimed at output. On the other hand, if conception increases, the resulting network training comes to an end. It will be optimal and augmented while attaining the mean absolute percentage deviation [MAPD]. It is also termed a mean squared error. The root mean square deviation will be premeditated with the average sum of the squared deviation between the actual value and the forecasted or estimated value characterised by the regression model (Upreti *et al.* n.d.) This is represented mathematically:

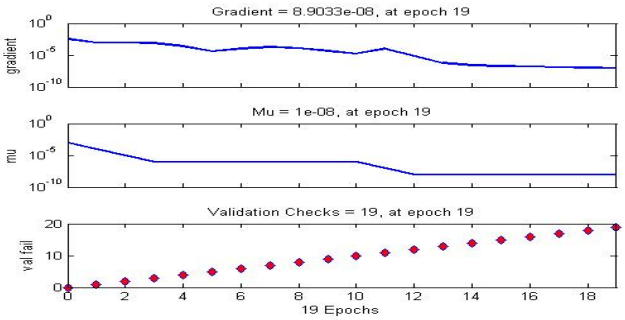

Overall status of the network for compressive strength

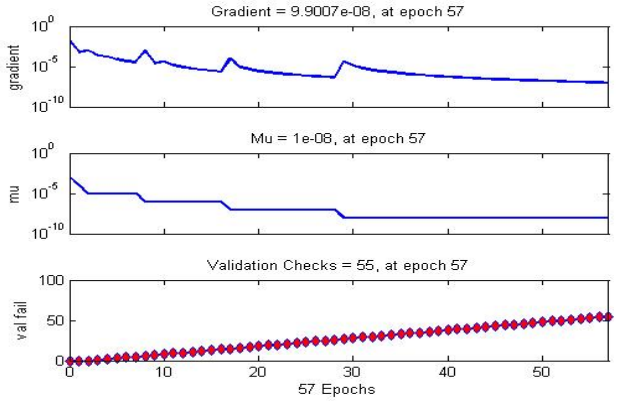

Overall status of the network for flexural strength

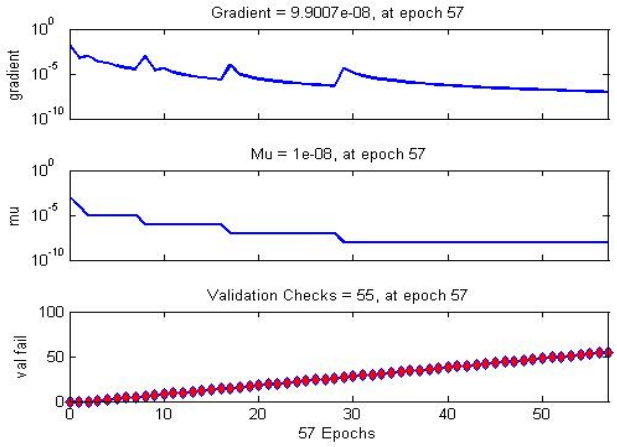

Overall status of the network for split tensile strength

Figure 17. Network overall status

The overall status of the network for compressive strength is shown in Figure17, with a lower MSE and R value indicating the best performance of the neural network model. Several trials were carried out with varying numbers of neurons, and the best result was obtained at the 7th epoch, which contained a single hidden layer with 12 neurons. Figure 17 illustrates the network's overall

status. To attain an artificial neural network model with an optimal result, the outcome was signified by the minimum mean absolute percentage deviation [MAPD] and coefficient of error. Innumerable evaluations with diverse neurons were made to get the optimal recital outcome, which could be at epochs having one hidden layer and 12 neurons at the seventh epoch. The overall network status is illustrated in Figure 17.

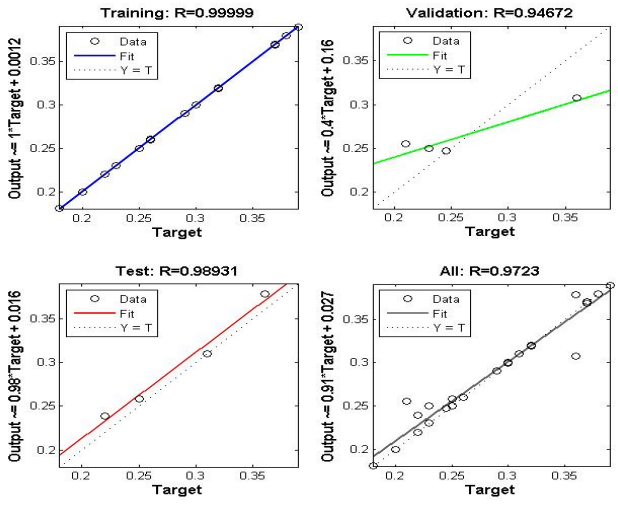

Compressive strength characterizes

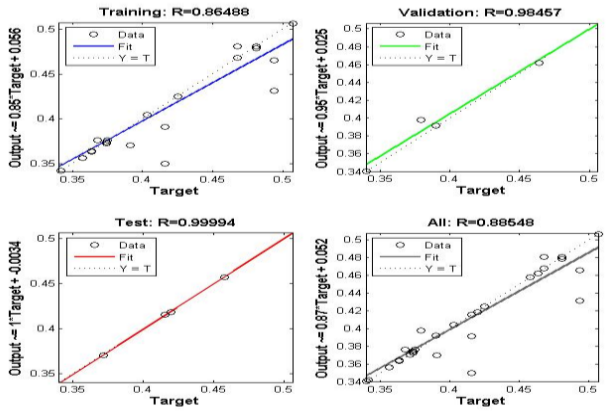

Flexure strength characterizes

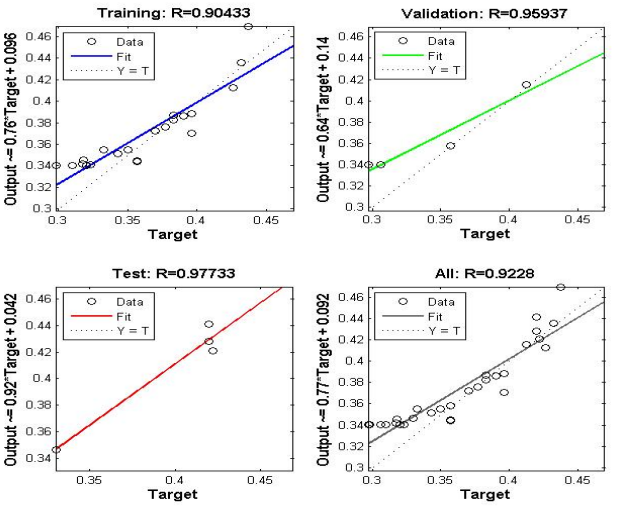

Split tensile strength characterises

Figure 18. Training, testing , validation and regression plots

Training, testing, and validation regression plots developed with MATLAB are illustrated in Figure 18. It was tried with a lot of iterations to make the coefficient of error reach the minimum value of zero, and the coefficient of error was premeditated. If the value of the coefficient of error is 1, that implies that the aimed input and output were very close in correction in the fitting of neurons. In this task, 10% of the data was deemed for testing, and the coefficient of error in testing was obtained as 0.998.

The developed network was trained to fit inputs and the targeted output. Training was done based on the train-back propagation algorithm. The network automatically stops training if generalisation stops improving. This is indicated by an increase in the mean squared error (MSE) value.

The mean squared error (R) is the average squared difference between the input and the targeted output. The R value shows the correlation between output and targets; if the R value is zero, there is no error. If the value of R = 1, then the relationship between targeted output and output obtained by the neural fitting tool is very close. 10% of the samples were considered for testing, and an R value of 0.989 was obtained for testing. An R value of 0.946 was obtained for validation. The regression plot of the network for training, testing, and validation is shown in Figure 18.

Figure 18 shows the regression plot of the training network for split tensile strength. 10% of the samples were considered for testing to predict the split tensile strength. An R value of 0.977 was obtained for testing. An R value of 0.959 was obtained for validation. From the outputs obtained, the model showed a higher coefficient of determination (> 0.9). The developed network was trained to fit inputs and the targeted output. Training was done based on the train-back propagation algorithm. The network automatically stops training if generalisation stops improving. This is indicated by an increase in the mean squared error (MSE) value.

6. Artificial neural network model validation

Artificial neural network models developed authoritative corroboration with the investigational outcome of results of diverse proportions of ingredients in geopolymer composites.

The mean absolute percentage deviation is calculated from the following Equation

$$RMSE = \sqrt{\frac{\sum_{i=1}^{N}\left(Predicted_i - Actual_i\right)^2}{N}}$$

The potential of the ANN model was evaluated with the potential parameters Root Mean Square Error (RMSE) and correction coefficient (R2) between the experimental results and the predicted results.

The compressive, flexural, and split tensile characteristic strengths of fly ash, M-sand, pond ash, and bottom ash as integrated geopolymer composites over 28 days were investigated, and the trial outcomes attained were evaluated and corroborated with ANN outcome prediction. Artificial neural network model predictions were compared

with trial outcomes of experimental results, and deviations in percentage as percentage error are illustrated in Table 12.

Table 12. Data of percentage error showing experimental result and ANN predicted result using ANN model

Mix Identity	Compressive strength characteristics (MPa)		% Error	Flexural strength characteristics (MPa)		% Error	Split tensile strength characteristics (MPa)		% Error
	trial outcome	ANN outcome prediction		trial outcome	ANN outcome prediction		trial outcome	ANN outcome prediction	
D-1	16.38	18.180	0.901	4.42	4.224	0.933	2.84	2.644	1.075
D -2	19.70	20.717	0.951	4.57	4.408	0.941	3.26	3.306	0.986
D -3	19.89	21.880	0.909	4.43	4.224	0.930	3.41	3.426	0.996
D -4	19.43	22.514	0.863	4.53	4.337	0.934	3.26	3.366	0.968
D -5	21.28	23.571	0.903	4.02	3.845	0.933	3.41	3.205	1.064
D -6	18.50	20.717	0.893	3.72	3.404	0.892	3.18	3.306	0.961
D -7	21.28	22.937	0.928	4.50	4.521	0.980	3.48	3.566	0.976
D -8	23.13	25.685	0.900	4.37	4.214	0.941	3.41	3.125	1.091
D -9	20.35	22.937	0.887	3.85	3.557	0.900	3.33	3.105	1.072
D -10	21.28	23.677	0.899	4.02	3.814	0.926	3.41	3.526	0.967
D -11	21.28	24.628	0.864	4.02	3.814	0.926	3.41	3.165	1.077
D -12	22.20	24.100	0.921	4.45	4.275	0.937	3.48	3.306	1.053
D -13	22.20	24.945	0.890	4.19	4.009	0.933	3.48	3.306	1.053
D -14	21.28	22.937	0.928	3.97	3.742	0.920	3.41	3.246	1.051
D -15	21.74	25.474	0.853	4.07	3.916	0.939	3.41	3.246	1.051
D -16	30.53	34.141	0.894	4.05	3.906	0.941	4.08	3.847	1.061
D -17	27.75	30.970	0.896	3.74	3.393	0.885	3.89	3.706	1.049
D -18	30.53	33.190	0.920	4.04	3.814	0.921	4.08	3.867	1.055
D -19	27.75	31.393	0.884	3.73	3.404	0.890	3.89	3.726	1.043
D -20	32.38	35.621	0.909	4.35	4.019	0.902	4.20	4.307	0.976
D -21	30.53	33.930	0.900	4.04	4.234	1.023	4.08	4.247	0.961
D -22	30.53	36.044	0.847	4.07	3.906	0.936	4.08	4.287	0.952
D -23	31.45	35.515	0.886	4.18	4.019	0.937	4.20	4.307	0.976
D -24	32.38	36.255	0.893	4.51	4.429	0.958	4.20	4.247	0.989
D -25	33.30	37.101	0.898	4.42	4.224	0.933	4.26	4.367	0.976
D -26	34.23	38.263	0.894	4.57	4.337	0.925	4.32	4.327	0.999
D -27	34.23	37.841	0.904	4.56	4.337	0.927	4.38	4.107	1.068
D -28	36.08	40.483	0.891	4.74	4.460	0.919	4.38	4.267	1.028
D -29	35.15	38.792	0.906	4.63	4.562	0.961	2.93	3.105	0.945
D -30	16.65	18.180	0.916	3.30	3.598	1.063	3.65	3.526	1.036
D -31	16.65	19.660	0.847	3.52	3.393	0.941	3.01	3.105	0.971
D -32	21.28	25.474	0.835	4.07	3.814	0.914	3.25	3.306	0.983
D -33	21.28	22.937	0.928	3.78	4.019	1.036	3.28	3.105	1.056
D -34	20.35	22.831	0.891	3.81	4.019	1.028	3.15	3.406	0.924
D -35	19.43	20.823	0.933	3.61	3.527	0.953	3.11	3.205	0.969
D -36	18.50	22.514	0.822	3.51	3.199	0.890	3.02	3.105	0.974
D -37	20.35	22.091	0.921	3.82	4.050	1.033	3.23	3.306	0.976
D -38	22.66	25.157	0.901	3.85	4.039	1.022	3.38	3.466	0.975
D -39	23.13	25.474	0.908	4.31	4.429	1.003	3.35	3.406	0.983
D 40	26.83	29.913	0.897	4.75	4.839	0.995	3.83	3.646	1.049
D -41	26.83	29.279	0.916	4.66	4.583	0.958	3.76	3.626	1.036
D -42	23.13	26.002	0.889	4.32	4.531	1.024	3.48	3.606	0.965
D -43	23.13	27.165	0.851	3.82	4.019	1.025	3.62	3.406	1.064
D -44	24.05	26.214	0.917	3.71	3.547	0.932	3.62	3.366	1.077
D -45	24.05	26.742	0.899	4.25	4.429	1.016	3.55	3.306	1.075
D -46	27.75	30.653	0.905	4.01	3.814	0.928	3.89	3.766	1.032
D -47	28.68	31.287	0.917	4.11	4.224	1.002	3.96	3.686	1.074
D -48	29.60	32.450	0.912	4.25	4.429	1.016	4.02	3.766	1.067
D -49	27.75	30.759	0.902	4.01	3.834	0.933	3.89	3.726	1.043
D -50	29.60	32.450	0.912	4.26	4.449	1.018	4.02	3.806	1.056

D -51	24.05	26.954	0.892	3.71	3.547	0.932	3.22	3.306	0.973
D -52	24.05	26.319	0.914	3.82	3.711	0.947	3.62	3.466	1.045
D -53	35.15	40.483	0.868	5.05	4.941	0.954	4.38	4.107	1.068
D -54	33.30	38.581	0.863	4.79	4.531	0.923	4.26	4.468	0.954
D -55	34.23	38.369	0.892	4.95	4.757	0.937	4.32	4.107	1.053
D -56	33.30	36.889	0.903	4.81	4.654	0.944	4.26	4.428	0.963
D -57	36.08	40.060	0.901	5.21	5.064	0.949	4.44	4.267	1.039
D -58	34.23	38.369	0.892	4.94	4.859	0.959	4.28	4.107	1.043
D -59	35.15	41.223	0.853	5.05	4.962	0.958	4.18	4.307	0.971
D -60	16.65	19.660	0.847	3.50	3.404	0.950	3.01	3.105	0.971
D -61	33.24	38.263	0.869	5.03	4.962	0.962	2.81	2.905	0.968
D -62	34.65	40.166	0.863	4.84	4.972	1.002	2.53	2.624	0.963
D -63	31.11	35.304	0.881	4.98	4.839	0.948	2.93	2.705	1.085
D 64	29.51	34.458	0.856	4.46	4.224	0.924	2.60	2.644	0.983
D -65	25.22	30.125	0.837	3.51	3.393	0.944	2.39	2.604	0.916
D -66	32.13	37.206	0.863	2.79	2.901	1.015	1.95	2.104	0.926
D -67	32.93	37.101	0.888	4.24	4.429	1.018	2.23	2.364	0.945
D -68	33.49	36.678	0.913	4.35	4.234	0.950	2.31	2.304	1.004
D -69	33.95	39.426	0.861	4.57	4.736	1.011	2.44	2.464	0.989
D -70	31.91	35.832	0.891	4.74	4.552	0.938	2.52	2.644	0.952

7. Results and Discussions

The number of neurons plays a vital role in the potential of the projected neural network, considering strength characterizes predictive replication, and it is crucial to choose the appropriate number of neurons for optimizing the recital level. Different statistics of neurons were used to appraise the effectiveness level of the projected network. The evaluation of the recital of the neural network with diverse numbers of neurons was prepared in terms of mean square error (MSE).

The data attained from the investigational test outcome was deemed the output for the artificial neural network model predictions, and the aimed output was explicit as compressive, flexural, and split tensile characteristic strengths in geopolymer composites attained from investigational corroboration [Zhong *et al.* 2024; Zhang *et al.* 2020].

Each discrete compressive, flexural, and split tensile characteristic strength of characteristics of fly ash, M-sand, pond ash, and bottom ash are integrated geopolymer composites investigation outcome result using the ANN model was predicted. The outcome of predicted flexural characteristic strength was correlated with authentic investigation outcome results, and the paramount curve athletic equation was evolved and illustrated in Figure 16. The prediction has been made for each and every individual compressive strength test result using the ANN model. The best curve fit equation has been developed between the predicted strength obtained from the ANN model and the actual compressive strength, as illustrated in Figure 16. The values obtained from experimentation and the values predicted from the ANN model were considered, and a regression plot was developed. The prediction was made for each and every individual flexural strength test result using the ANN model. The best curve fit equation was developed between the predicted characteristic strength obtained from the ANN model and the actual flexural characteristic strength, as illustrated in Figure 19. It is worth mentioning that all these models are constructed to investigate the efficiency of each individual input parameter on the output value. Overall, the developed ANN model is more satisfactory in predicting the 28-day compressive, flexural, and split tensile characteristic strengths of fly ash, M-sand, pond ash, and bottom ash as integrated geopolymer composites.

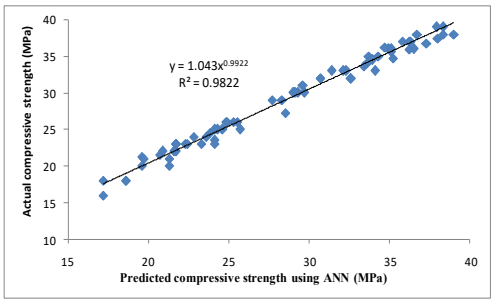

Predicted strength by ANN vs actual compressive strength

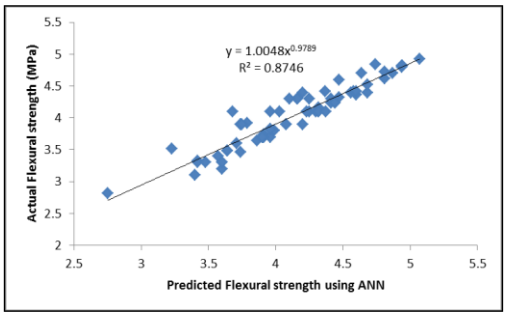

Predicted flexural strength by ANN vs actual flexural strength

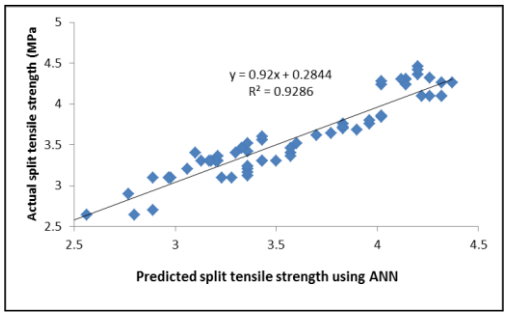

Predicted flexural strength by ANN vs actual split tensile strength

Figure 19. Discrete Strength Characteristic Strength Vs Outcome by ANN Characteristic Strength

In the paramount curve, an athletic equation evolved with a correlation coefficient of 0.982, with outcome results using the ANN model predicted and compressive, flexural, and split tensile characteristic strength investigation outcome results. It is shown that the coefficient determined to establish strength inference is within a close range of the ANN values found with the experimental outcome. Though plenty of expertise is available for predicting the compressive, flexural, and split tensile characteristic strengths of geopolymer composites, the most effective device is artificial neural network model prediction. Figure 19 illustrates the best validation performance of the neural network for flexural strength.

The correlation coefficient of 0.982 was obtained for the best A curve fit equation is plotted between the predicted strength characteristics obtained from ANN model and the actual compressive strength characteristics. The coefficient of determination shows the strength characteristics prediction is very close to the actual values obtained from the test results. Among the numerous techniques available to predict the strength characteristics of geopolymer composites, ANN is considered the most effective tool. Figure 19 shows the best validation performance of the network and the best validation performance of the neural network for flexural strength characteristics. 10% of the samples were considered for testing to predict the flexural strength characteristics. An R value of 0.999 was obtained for testing. An R value of 0.984 was obtained for validation. Figure 20 shows the best validation performance of the neural network for flexural strength characteristics. 10% of the samples were considered for testing to predict the flexural strength characteristics. An R value of 0.999 was obtained for testing. An R value of 0.984 was obtained for validation. Figure 20 illustrates the best validation performance of a neural network for split tensile strength characteristics. The correlation coefficient of 0.928 was obtained for the best curve fit equation plotted between the predicted strength characteristics obtained from the ANN model and the actual split tensile strength. The coefficient of determination shows the strength prediction was very close to the actual values obtained from the test results. The best curve fit equation has been developed between the predicted strength characteristics obtained from the ANN model and the actual split tensile strength characteristics, as illustrated in Figure 20.

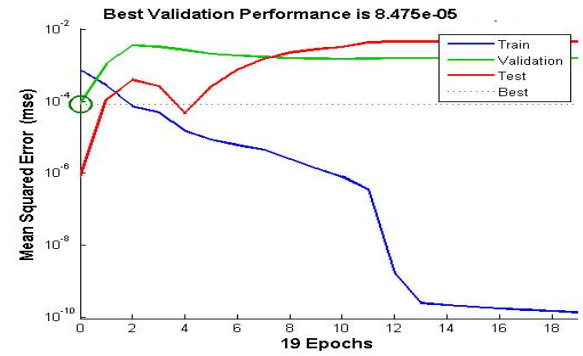

The best validation performance of the neural network for compressive strength

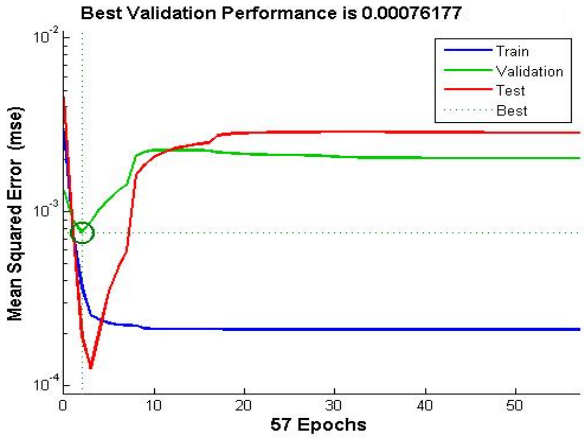

The best validation performance of the neural network for flexural strength

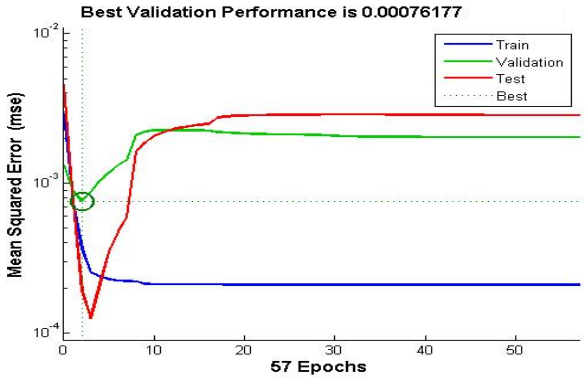

The best validation performance of the neural network for split tensile strength

Figure 20. The best validation performance of the neural network

In this work, artificial neural network modelling was done for a geopolymer composite incorporating fly ash, pond ash, manufactured sand, and bottom ash. In this paper, for the prediction of the outcome of compressive, flexural, and split tensile characteristic strength characteristics, 70 trial values were put into use. The outputs obtainable are appreciably precise, and error is diminished.

8. Conclusion

By exploiting Levenberg-Marquardt algorithms, an artificial neural network model was evolved to predict the compressive, split tensile, and flexural strength potentials of geopolymer composites by applying experimentation

data. By exploiting the data obtained by carrying out experiments and assessments, input and output models were trained. Being Levenberg-Marquardtalgorithm more precise output obtained were better reliable , correct very closer to the investigational data with tiny errors strength potentials of geopolymer composite. ANNs were employed in this study to predict the compressive strength of geocomposite, and the prediction accuracy was validated. Hence, strength characteristics can be predicted with artificial neural networks without carrying out any testing. It may have had the highest error from -0.0029 to 0.0034 when evaluating the assessment achieved from the testing. These values of RMSE and R2 corroborate that the employment of ANN for the prediction of strength characteristics is an excellent option due to its tremendous correlation with the investigational outcome .The geopolymer composite is produced by blending fly ash, pond ash, manufactured sand, and bottom ash as diverse ingredient factors affecting its strength. The geopolymer composite, with its optimized parameters, provides sufficient strength. Geopolymer composite is superfluous, ecologically pleasurable, and has the ability to replace standard cement concrete in plenty of projects that contain precast gadgets. Hence, it is applicable as a composite in construction works by exploiting industrial byproducts. This study suggests that ANNs are an effective tool in strength prediction of geocomposites, reducing further the experimental cost and time.

Declarations

Funding declaration

Funding is “not applicable” since funding was received.

Conflicts of interest or competing interests

The authors declare that they have no known competing financial interests or personal relationships that could have appeared to influence the work reported in this paper. “no conflicts of interest.”

Author contribution declaration

Conceptualization: RajagopalShanmugam Methodology: Rajendran Selvapriya Formal analysis and investigation: Rajendran Selvapriya, Paramasivam Tamilchelvan, Murugesan Gopinath Writing: original draft preparation: ParamasivamTamilchelvan, Writing, review, and editing: Murugesan Gopinath Funding Acquisition: NA, Resources: Rajagopal Shanmugam, Rajendran Selvapriya, Paramasivam Tamilchelvan, Murugesan Gopinath Supervision: RajagopalShanmugam

All authors have read and agreed to the published version of the manuscript.

Data availability

Data is available on request from the authors.

Acknowledgement

NIL

10. References

Adesanya E, Aladejare A, Adediran A, Lawal A, Illikainen M. Predicting shrinkage of alkali-activated blast furnace-fly ash mortars using artificial neural network (ANN). Cement and Concrete Composites. 2021 Nov 1;124:104265.

Anuradha, R., V. Sreevidya, R. Venkatasubramani, and B. Vijaya Rangan. "Modified guidelines for geopolymer concrete mix design using Indian standard." (2012): 357-368.

Ahmed HU, Abdalla AA, Mohammed AS, Mohammed AA, Mosavi A. Statistical methods for modeling the compressive strength of geopolymer mortar. Materials. 2022 Mar 2;15(5):1868.

Ahmed HU, Mohammed AS, Mohammed AA. Proposing Several Model Techniques Including ANN and M5P-tree to Forecast the Stress at the Failure of Geopolymer Concrete Mixtures Incorporated Nano-silica.

Alakara EH, Nacar S, Sevim O, Korkmaz S, Demir I. Determination of compressive strength of perlite-containing slag-based geopolymers and its prediction using artificial neural network and regression-based methods. Construction and Building Materials. 2022 Dec 12; 359: 129518.

Bhogayata A, Kakadiya S, Makwana R. Neural Network for Mixture Design Optimization of Geopolymer Concrete. ACI Materials Journal. 2021 Jul 1;118(4).

Barbuta M, Diaconescu RM, Harja M. Using neural networks for prediction of properties of polymer concrete with fly ash. Journal of Materials in Civil Engineering. 2012 May 1;24(5):523-8.

Cong P, Cheng Y. Advances in geopolymer materials: A comprehensive review Journal of Traffic and Transportation Engineering (English Edition). 2021 Jun 1;8(3):283-314.

Durga ml, reddy pn, sumanth ts, devi ay, kumar bs, kumar ms. Predicting the strength of ggbs based geopolymer concrete by using artificial neural networks

Emami S, Kamalloo A. Enhancing mechanical strength of inorganic geopolymer by using phenol resin. International Journal of Engineering. 2012 Nov 1;25(4):325-8.

Gupta P, Gupta N, Saxena KK, Goyal S. Multilayer perceptron modelling of geopolymer composite incorporating fly ash and GGBS for prediction of compressive strength. Advances in Materials and Processing Technologies. 2022 Oct 31;8(sup3):1441-55.

Gunasekara C, Atzarakis P, Lokuge W, Law DW, Setunge S. Novel analytical method for mix design and performance prediction of high calcium fly ash geopolymer concrete. Polymers. 2021 Mar 15;13(6):900.

Lau CK, Lee H, Vimonsatit V, Huen WY, Chindaprasirt P. Abrasion resistance behaviour of fly ash based geopolymer using nanoindentation and artificial neural network. Construction and Building Materials. 2019 Jul 10;212:635-44.

Karimipour A, Abad JM, Fasihihour N. Predicting the load-carrying capacity of GFRP-reinforced concrete columns using ANN and evolutionary strategy. Composite Structures. 2021 Nov 1;275:114470. Khan K, Iqbal M, Salami BA, Amin MN, Ahamd I, Alabdullah AA, Arab AM, Jalal FE.Estimating Flexural Strength of FRP Reinforced Beam Using Artificial Neural Network and Random Forest Prediction Models. Polymers. 2022 Jun 2;14(11):2270

Kuppusamy Y, Jayaseelan R, Pandulu G, Sathish Kumar V, Murali G, Dixit S, Vatin NI. Artificial Neural Network with a Cross-Validation Technique to Predict the Material Design of Eco-

Friendly Engineered Geopolymer Composites. Materials 2022, 15, 3443.

Kong YK, Kurumisawa K. Prediction of the drying shrinkage of alkali-activated materials using artificial neural networks. Case Studies in Construction Materials. 2022 Dec 1;17:e01166.

Manikandan P, Vasugi V. The potential use of waste glass powder in slag-based geopolymer concrete-an environmentally friendly material. International Journal of Environment and Waste Management. 2023;31(3):291-307.

Nagajothi S, Elavenil S. Influence of aluminosilicate for the prediction of mechanical properties of geopolymer concrete–artificial neural network. Silicon. 2020 May;12(5):1011-21.

Pratap B, Shubham K, Mondal S, Rao BH. Exploring the potential of neural network in assessing mechanical properties of geopolymer concrete incorporating fly ash and phosphogypsum in pavement applications. Asian Journal of Civil Engineering. 2023 May 30:1-5.

Peng Zhang a b, Zhen Gao a, Juan Wang a, Jinjun Guo a b, Tingya Wang a Influencing factors analysis and optimized prediction model for rheology and flowability of nano-SiO2 and PVA fiber reinforced alkali-activated composites Journal of Cleaner Production, Volume 366, 15 September 2022, 132988

Rehman F, Khokhar SA, Khushnood RA. ANN based predictive mimicker for mechanical and rheological properties of eco-friendly geopolymer concrete. Case Studies in Construction Materials. 2022 Dec 1;17:e01536.

Sharma U, Gupta N, Verma M. Prediction of the compressive strength of Flyash and GGBS incorporated geopolymer concrete using artificial neural network. Asian Journal of Civil Engineering. 2023 May 1:1-4.

Sakthieswaran N, Dhanaraj R, Suresh P. copper slag-silica fume blended fibre concrete–an eco-friendly healthy alternative for conventional cement concrete. revista romana de materiale. 2020;50(1):81-9.

Ting-Yu LiuPeng ZhangJuan WangYi-Feng Ling Compressive Strength Prediction of PVA Fiber-Reinforced Cementitious Composites Containing Nano-SiO2 Using BP Neural Network Materials 2020

Tingyu Liu a, Peng Zhang a, Guo Cui b, Xiaodong Yue b Fracture performance prediction of polyvinyl alcohol fiber-reinforced cementitious composites containing nano-SiO2 using least-squares support vector machine optimized with quantum-behaved particle swarm optimization algorithm Theoretical and Applied Fracture Mechanics Volume 115, October 2021, 103074

Upreti K, Verma M. Prediction of Compressive Strength of Geopolymer Concrete using Artificial Neural Network.

Wang Q, Ahmad W, Ahmad A, Aslam F, Mohamed A, Vatin NI. Application of soft computing techniques to predict the strength of geopolymer composites. Polymers. 2022 Mar 8;14(6):1074.

Yadollahi MM, Benli A, Demirboğa R. Prediction of compressive strength of geopolymer composites using an artificial neural network. Materials Research Innovations. 2015 Sep 19;19(6):453-458.

Yaswanth KK, Revathy J, Gajalakshmi P. Soft computing techniques for the prediction and analysis of compressive strength of alkali-activated Alumino-silicate based strain-hardening Geopolymer composites. Silicon. 2022 Apr:1-24.

Zhang B, Zhu H, Feng P, Zhang P. A review on shrinkage-reducing methods and mechanisms of alkali-activated/geopolymer systems: Effects of chemical additives. Journal of Building Engineering. 2022 May 15;49: 104056.

Zhong W.L., H. Ding, X. Zhao, L.F. Fan Mechanical properties prediction of geopolymer concrete subjected to high temperature by BP neural network Construction and Building Materials Volume 409, 15 December 2023**,**

Zhong W.L., B. Qiu, Y.H. Zhang, X. Zhao, L.F. FanMesoscopic damage characteristics of hydrophobicity-modified geopolymer composites under freezing-thawing cycles based on CT scanningComposite StructuresVolume 326, 15 December 2023, 117637

Zhong W.L., L.F. Fan, Y.H. ZhangExperimental research on the dynamic compressive properties of lightweight slag based geopolymer Ceramics International Volume 48, Issue 14, 15 July 2022, Pages 20426-20437

Zhong W.L., Zhang Y.H., Fan L.F. High-ductile engineered geopolymer composites (EGC) prepared by calcined natural clay Journal of Building EngineeringVolume 63, Part A, 1 January 2023,

Zhong W.L., Zhang Y.H., Fan L.F., Li P.F. Effect of PDMS content on waterproofing and mechanical properties of geopolymer composites Ceramics International Volume 48, Issue 18, 15 September 2022, Pages 26248-26257

Zhong W.L., Sun Y.H., Zhao X., Fan L.F. Study on synthesis and water stability of geopolymer pavement base material using waste sludge Journal of Cleaner Production. Volume 445, 15 March 2024, 141331

Zhang P, Wang K, Wang J, Guo J, Hu S, Ling Y. Mechanical properties and prediction of fracture parameters of geopolymer/alkali-activated mortar modified with PVA fiber and nano-SiO2. Ceramics International. 2020 Aug 15; 46(12):20027-37.

Zhen Gao, Peng Zhang, Jinjun Guo, Kexun Wang Bonding behavior of concrete matrix and alkali-activated mortar incorporating nano-SiO2 and polyvinyl alcohol fiber: Theoretical analysis and prediction model Ceramics International Volume 47, Issue 22, 15 November 2021, Pages 31638-31649